Available online at www.sciencedirect.com
ScienceDirect
Journal of Catalysis 254 (2008) 1–11
JOURNAL OF CATALYSIS
www.elsevier.com/locate/jcat

Kinetics and mechanism of ethylene hydrogenation poisoned by CO on silica-supported monodisperse Pt nanoparticles

Robert M. Rioux [1], Russell Komor [2], Hyunjoon Song [3], James D. Hoefelmeyer [4], Michael Grass, Krisztian Niesz [5], Peidong Yang, Gabor A. Somorjai *

Department of Chemistry, University of California, Berkeley and Lawrence Berkeley National Laboratory, Materials and Chemical Sciences Divisions, Berkeley, CA 94720, USA

Received 28 August 2007; revised 14 October 2007; accepted 20 October 2007

Available online 26 December 2007

Abstract

The influence of particle size on the poisoning of ethylene hydrogenation by CO was studied over a series of catalysts composed of nearly monodisperse Pt nanoparticles (1.7–7.1 nm) encapsulated in mesoporous silica (SBA-15). The turnover frequency at 403 K in the presence of 0.5 Torr CO was $\sim 2 \times 10^{-2}$ s^{-1} (compared with $\sim 10^{2}$ s^{-1} in the absence of CO). The apparent activation energy in the absence and presence of 0.2 Torr CO was ~10 and 20 kcal mol^{-1}, respectively. The pressure dependency changes significantly in the presence of CO; reaction orders in hydrogen were 1/2 in the presence of CO at 403 K and noncompetitive with regard to co-adsorption with C_2H_4. In the absence of CO at similar temperatures, H_2 adsorption was primarily irreversible (first-order dependence), and H_2 and C_2H_4 compete for the same sites. Ethylene orders at 403 K were first order in the presence of 0.2 Torr CO and remained unity with increasing CO pressure. At similar reaction conditions in the absence of CO, ethylene had an inhibitory effect (negative reaction order) on the overall hydrogenation reaction. The change in C_2H_4 and H_2 kinetics suggests strong competitive adsorption between C_2H_4 and CO for the same type of site, whereas H_2 apparently adsorbs on distinct surface sites due either to steric hindrance or H_2-induced CO desorption. Incorporation of a quasi-equilibrated CO adsorption step into a noncompetitive Langmuir–Hinshelwood mechanism predicts the experimentally observed pressure dependencies and a doubling of the apparent activation energy. Hydrogenation of ethylene in the presence of 1 Torr CO was examined under reaction conditions at 403 K by infrared spectroscopy; the only surface species identified under reaction conditions was linear-bound CO. The hydrogenation of ethylene on clean Pt catalysts was structure-insensitive and remains insensitive in the presence of CO; rates decreased only by a factor of two with increasing particle size.

Keywords: Pt; Nanoparticles; Monodisperse; Ethylene hydrogenation; CO; Poisoning; Kinetics; Mechanism; Structure insensitivity

1. Introduction

Designing heterogeneous catalysts that are capable of the highest possible selectivity at relevant conversions under environmentally benign conditions is an important research objective in heterogeneous catalysis. Toward that end, the design and synthesis of high-surface area Pt catalysts with tunable parameters (i.e., particle size and/or shape) has been pursued [1–3]. Monodisperse platinum nanoparticles are synthesized by solution-based reduction methods [2,4,5], followed by encapsulation of the nanoparticles in the pores of a mesoporous SBA-15 silica matrix [3]. The properties of these catalysts can be tuned systematically to understand the influence of

* Corresponding author.
E-mail address: somorjai@berkeley.edu (G.A. Somorjai).
[1] Current address: Department of Chemistry and Chemical Biology, Harvard University, Cambridge, MA 02138, USA.
[2] Current address: Department of Chemical Engineering, California Institute of Technology, Pasadena, CA 91125, USA.
[3] Current address: Department of Chemistry and School of Molecular Science (BK21), Korea Advanced Institute of Science and Technology, Daejeon, 305-701, Korea.
[4] Current address: Department of Chemistry, University of South Dakota, Vermillion, SD 57069, USA.
[5] Current address: ThalesNano Inc., Zahony u. 7, H-1031, Budapest, Hungary.

0021-9517/$ – see front matter
doi:10.1016/j.jcat.2007.10.015

catalyst structure on catalytic activity [1–3]. Detailed control of morphology enables the investigation of structure–function (activity and selectivity) relationships, and also enables the elucidation of surface structure (i.e., particle size) on the resistance of a catalyst to poisoning/deactivation resistance.

The mechanism by which an adsorbate poisons a catalytic reaction is site blocking, perturbation of the surface electronic structure (by either charge screening or surface reconstruction), or a combination of both. The mechanistic complexity of poisoning is tractable when the influence of a poison is examined during a well-studied reaction; an example is the influence of CO poisoning on olefin conversion reactions [6–10]. Suppression of turnover frequency (TOF) is severe in some cases; whereas other catalysts appear resistant to poisoning by CO [8–10]. CO is one of the most widely studied adsorbates because it serves as an indicator of local surface structure [11,12], making it an ideal probe molecule for investigating the influence of particle size on poison resistance. The CO stretching frequency is sensitive to the identity of neighboring adsorbates [13] and may provide insight into the interaction between poison and reactant molecules on the catalyst surface. CO adsorption perturbs the electronic structure of the surface Pt atoms by significant donation from the 2p orbital into the metal d-orbital and back-donation to the anti-bonding $2\pi^*$ orbital of adsorbed CO [14]. Strong adsorption of CO on Pt surfaces predisposes it to compete for sites and inhibit turnover during olefin conversion reactions. The co-adsorption of CO and ethylene on monodisperse Pt(X)/SBA-15 ($X = 1.7$, 2.9, 3.6, and 7.1 nm) catalysts was studied by volumetric adsorption measurements and infrared spectroscopy [15]. The results of study demonstrated that CO and ethylene compete directly for surface sites. Co-adsorption experiments revealed that the composition of the surface layer is dependent on the order gas of exposure. CO adsorbs on an ethylene-covered surface, although modified by its presence; however, in the case of ethylene adsorption on a CO-covered surface, the adsorption of ethylene is eliminated almost completely.

In this paper, the hydrogenation of ethylene in the presence of 0.2–1 Torr CO was examined on Pt/SBA-15 catalysts. Kinetic measurements demonstrated that the ethylene hydrogenation rate decreased by ∼4 orders of magnitude on the addition of 0.5 Torr CO at 403 K. Kinetic parameters were influenced by the presence of CO; the most notable change was a doubling of the apparent activation energy in the presence of CO. The sequence of elementary steps proposed for the noncompetitive Horiuti–Polanyi mechanism [16] with the inclusion of an equilibrated CO adsorption step enables formulation of a rate expression that captures the experimentally observed kinetics. This work demonstrates that the rate of olefin hydrogenation, which is insensitive to the size of the metal nanoparticles in the absence of CO, remains structure-insensitive in the presence of CO, even though the adsorption of CO is sensitive to the catalyst structure.

2. Experimental

2.1. Catalyst synthesis and characterization

The synthesis and characterization of catalysts used in this study have been described in detail previously [2,3] and here discussed briefly. Pt particles were synthesized according to literature methods [4,5]. The 1.7-nm Pt particles were synthesized by adding NaOH solution (12.5 mL, 0.5 M) in ethylene glycol (EG) to a solution of dihydrogen hexachloroplatinate ($H_2PtCl_6{\cdot}6H_2O$, Alfa Aesar, 250 mg) in 12.5 mL of EG. The mixture was heated at 433 K for 3 h with bubbling N_2. After reaction, particles were precipitated by the addition of 2 M HCl (1 mL) and dispersed in ethanol containing 12.2 mg of poly(vinylpyrrolidone) (PVP; $M_w = 29{,}000$; Sigma-Aldrich). The 2.9-nm particles were synthesized by refluxing a mixture of PVP (266 mg) and $H_2PtCl_6{\cdot}6H_2O$ (124.3 mg) in a water (40 mL)–methanol (360 mL) solution for 3 h. The 3.6-nm Pt particles were formed by mixing the 2.9-nm Pt colloidal solution (100 mL) in a water/methanol (1:9) mixture with 10 mL of 6.0 mM $H_2PtCl_6{\cdot}6H_2O$ aqueous solution and 90 mL of methanol, followed by refluxing for 3 h. The 7.1-nm Pt particles were synthesized by adding 93.8 μL of 0.375 M PVP ($M_w = 55{,}000$, Sigma-Aldrich) and 46.9 μL of 62.5 mM $H_2PtCl_6{\cdot}6H_2O$ solutions EG at reflux every 30 s over 16 min, followed by an additional 5 min reflux [17]. Pt colloidal solutions were purified by sequential precipitation/redispersion and dispersed in an appropriate amount of deionized water to make a 3×10^{-3} M solution (based on Pt salt concentration). Estimated particle sizes were 1.73 ± 0.26 (1.7), 2.80 ± 0.21 (2.9), 3.39 ± 0.26 (3.6), and 7.16 ± 0.37 (7.1) nm by transmission electron microscopy (TEM) and X-ray diffraction (XRD) (in parentheses), indicating high uniformity and monodispersity of each particle smaller than $\sigma \sim 8\%$ [2].

The synthesis of Pt(X)/SBA-15 catalysts by the nanoparticle encapsulation (NE) method has been reported previously [3]. Pluronic P123 (2.5 g, $EO_{20}PO_{70}EO_{20}$, BASF) was completely dissolved in deionized water (50.5 mL). The Pt colloidal aqueous solution (27.0 mL, 3×10^{-3} M) was mixed with the polymer solution and stirred for 1 h at 313 K. Then 0.375 mL of 0.5 M NaF aqueous solution was added, and 3.91 mL of tetramethyl orthosilicate (TMOS, 98%, Aldrich) was quickly added to the reaction mixture, followed by stirring for a day at 313 K. The resulting slurry was aged for an additional day at 373 K. The brown precipitate was separated by centrifugation, thoroughly washed with ethanol, and dried in an oven at 373 K. The Pt(1.7 nm)/SBA-15 was calcined at 623 K for 24 h, the Pt(7.1 nm)/SBA-15 was calcined at 723 K for 36 h, and the 2.9 and 3.6-nm catalysts were calcined at 723 K for 24 h. Typically, 300–400 mg of Pt(X)/SBA-15 was calcined in a horizontal tube furnace at the specified temperature and time in 100 mL (NTP) min^{-1} of 20% O_2/He (both gases ultra-high purity (UHP), Praxair). Calcined samples were stored in scintillation vials before use.

A 3.2% Pt/SiO_2 catalyst prepared by ion exchange of $Pt(NH_3)_4(OH)_2{\cdot}xH_2O$ [18] and a UHP Pt powder (Alfa Aesar, 1 μm particle size) were used as standards for reaction stud-

ies. The UHP Pt powder was cleaned by heating at 473 K for 0.5 h in 10% O_2/He to remove any surface contaminants before normal catalyst pretreatment. A 2% Pt/Al_2O_3 (Exxon Research and Engineering) also was included in this study to investigate whether the support influenced the poisoning of ethylene hydrogenation by CO. All standard catalyst samples were reduced at 673 K by the same procedure used for the SBA-15 catalysts [2,3].

XRD spectra were measured on a Bruker D8 GADDS diffractometer using Co$K\alpha$ radiation (1.79 Å). Selective gas adsorption measurements were conducted in a Pyrex volumetric apparatus pumped by a liquid nitrogen–cooled diffusion pump to sample cell pressures of $\leqslant 3 \times 10^{-6}$ Torr. Total and reversible isotherms were collected at room temperature, with an interim 1 h evacuation between isotherms. Monolayer uptakes were determined by extrapolating adsorbate uptakes to zero pressure. Catalysts were reduced for 75 min at 673 K in 50 mL (NTP) H_2 min^{-1} (Praxair, UHP, 99.999%), followed by evacuation at 623 K before beginning the adsorption measurements.

2.2. Kinetic measurements of C_2H_4 hydrogenation in the presence and absence of CO

Kinetic measurements were conducted in a quartz plug-flow reactor (PFR) operating under differential conditions. Conversions were maintained below 5% for most catalysts. Pt/SBA-15 catalysts (10–50 mg) diluted in acid-washed low-surface area quartz (∼50–250 mg) (Aldrich) were reduced by the same pretreatment protocol used for chemisorption samples. He (Praxair, UHP, 99.999%), H_2 (Praxair, UHP, 99.999%), C_2H_4 (AirGas, CP grade), and CO (Matheson, UHP, Al cylinder) were delivered to the reactor with mass-flow controllers (Unit Instruments Corporation, model UFC 1200) at a total flow rate of 90 mL (NTP) min^{-1}. Reactant and product concentrations were measured by a gas chromatograph (Hewlett Packard 5890 series II) equipped with a 10-way sampling valve that allows simultaneous monitoring of C_2H_4 and C_2H_6 with a flame ionization detector (FID) and CO and H_2 with a thermal conductivity detector (TCD). All TOF values (corrected to standard conditions of 10 Torr C_2H_4, 100 Torr H_2, 0.5 Torr CO and 403 K) were reproducible to ±10% (determined by multiple measurements) and calculated using the dispersion from the total H_2–O_2 uptake [18]. No conversion of CO to methane through a CO/H_2 reaction was detected.

2.3. In situ infrared spectroscopy measurements of C_2H_4 hydrogenation in the absence and presence of CO

In situ diffuse–reflectance infrared Fourier transform spectroscopy (DRIFTS), using a Nicolet Nexus 670 spectrometer equipped with a Thermo Spectra-Tech controlled-atmosphere diffuse reflectance cell, was used to study the reaction between ethylene and hydrogen in the presence of CO at 403 K. The IR cell was operated at conditions similar to those used for microreactor studies. Typically, a Pt/SiO_2 catalyst (ca. 50 mg amorphous SiO_2, ca. 20–30 mg SBA-15 samples) was loaded into the cell and subjected to an identical pretreatment as used for the catalytic studies with a gas-handling manifold equipped with mass flow controllers (Porter Instruments Co.) connected to the diffuse reflectance cell. He (99.999%, Praxair), H_2 (99.999%, Praxair), CO (99.9%, AirGas), and C_2H_4 (99.9%, Praxair) were used without further purification. Single-beam spectra (128 scans, 2 cm^{-1} resolution) of the freshly reduced catalyst were obtained at 300 or 403 K under 30 mL (NTP) He min^{-1} and used to subtract silica features from *in situ* spectra. Samples were heated to reaction temperature (300 or 403 K) in He and then exposed to a 90 mL (NTP) min^{-1} mixture of 10 Torr C_2H_4, 100 Torr H_2, and 1 Torr CO (which, because of experimental constraints, was the lowest obtainable CO pressure). Separately, a spectrum of gas-phase CO (1 Torr) and ethylene (10 Torr) obtained in the DRIFTS cell using a Au mirror was subtracted from the *in situ* spectrum. The only results presented herein are for a 2.69% Pt(2.9 nm)/SBA-15 catalyst, which is representative of all samples.

3. Results

3.1. Catalyst characterization

The characterization of the Pt(X)/SBA-15 series catalysts has been reported previously [2,3]. The X nomenclature in Pt(X)/SBA-15 represents the size of the free-standing (unsupported) nanoparticle determined by TEM [2]. Catalysts were prepared with a nominal weight loading of 1%; actual metal loadings determined by elemental analysis (inductively-coupled plasma optical emission spectroscopy (ICP-OES); Galbraith Laboratories, Knoxville, TN) were between 0.6 and 0.8 wt%. Estimation of particle size based on XRD was not successful because of the low signal-to-noise ratio of the Pt Bragg reflections. Only in the case of the Pt(7.1 nm)/SBA-15 catalyst could a particle size be determined (Table 1).

Removal of PVP from encapsulated nanoparticle surfaces is achieved by sample-dependent long calcination times (24–36 h) at relatively high temperatures (623–673 K). Selective gas adsorption (H_2–O_2 chemisorption) measurements of the exposed Pt surface area are summarized in Table 1.

3.2. Kinetics of C_2H_4 hydrogenation on Pt/SBA-15 catalysts poisoned by CO

The kinetics of C_2H_4 hydrogenation in the presence of CO (0.2–0.9 Torr) was studied over a series of SBA-15 supported Pt catalysts. In the absence of CO, the TOF for ethylene hydrogenation is $\sim 10^2$ s^{-1} at 403 K, while the catalytic activity varied from 1.7–3.5 $\times 10^{-2}$ s^{-1} at 10 Torr C_2H_4, 100 Torr H_2, 0.5 Torr CO, and 403 K. The activity (per gram catalyst) and TOFs are reported in Table 2. TOFs were reproducibly higher on the Pt(1.7 nm)/SBA-15 and 2% Pt/Al_2O_3, two samples with the same particle size (∼2.7 nm), as determined by H_2–O_2 titration. The difference in TOF varied by only a factor of two over the entire particle size range studied (1–290 nm); in the presence of CO, ethylene hydrogenation is considered structure-

Table 1
Adsorption uptake and particle size determined by chemisorption and XRD

Catalyst[a,b]	Probe gas uptakes[c] (μmol g^{-1})					Dispersion, D	Particle size, d (nm)		
	H_2	CO		O_2	H_2–O_2	H_2–$O_{2,total}$	Chemisorption[d]		XRD[e]
	total	Total	Irrev.	irrev.	total		H_2	H_2–O_2	
3.2% Pt/SiO_2-IE	133.1	166.7	152.2	24.2	262.0	1[f]	1.0	1.0	–[g]
2% Pt/Al_2O_3-Exxon	43.5	80.6	70.1	17.4	66.1	0.43	1.3	2.6	–[g]
0.6% Pt(1.7 nm)/SBA-15	4.5	13.3	12.0	4.4	19.1	0.416	3.8	2.7	–[g]
0.77% Pt(2.9 nm)/SBA-15	6.0	11.3	10.0	4.4	21.8	0.368	3.7	3.1	–[g]
0.6% Pt(3.6 nm)/SBA-15	4.0	7.9	7.4	3.1	12.5	0.270	4.4	4.2	–[g]
0.62% Pt(7.1 nm)/SBA-15	1.5	2.9	2.3	2.4	5.6	0.117	11.9	9.4	7.8
UHP Pt powder	16.7	15.1	13.7	8.6	30.3	0.004	173.5	286.5	>100

[a] Elemental analysis determined by ICP-OES.
[b] Number average particle size determined by TEM. Determined by counting a minimum of 200 free-standing particles.
[c] Conducted at 295 K.
[d] Determined from $1.13/(Pt_s/Pt_T)$.
[e] Based on the Scherrer–Debye equation after subtracting SBA-15 baseline.
[f] Dispersion calculated >1, assumed $D = 1$ for turnover frequency calculations.
[g] Not detectable.

Table 2
Ethylene hydrogenation reaction kinetics on supported Pt catalysts in the presence of CO

Catalyst[a]	Kinetic parameters in the presence of CO					
	Activity[b] (μmol g^{-1} s^{-1})	TOF[b,c] (×100 s^{-1})	E_a[d] (kcal mol^{-1})	Reaction orders		
				C_2H_4[e]	H_2[f]	CO[g]
3.2% Pt/SiO_2-IE	3.2	2.0	20.3	0.89	0.67	−1.1
2% Pt/Al_2O_3-Exxon	1.5	3.5	22.1	0.88	0.62	−1.1
0.6% Pt(1.7 nm)/SBA-15	0.43	3.4	21.6	0.97	0.60	−1.2
0.77% Pt(2.9 nm)/SBA-15	0.38	2.7	20.1	0.96	0.52	−1.1
0.6% Pt(3.6 nm)/SBA-15	0.19	2.3	20.7	0.99	0.44	−1.1
0.62% Pt(7.1 nm)/SBA-15	0.06	1.7	22.0	0.98	0.46	−1.0
UHP Pt powder	0.39	2.0	13.6	1	0.44	−1.1

[a] Actual Pt weight loading determined by ICP-OES.
[b] Rates corrected to 10 Torr C_2H_4, 100 Torr H_2, 0.5 Torr CO and 403 K.
[c] Based on number of surface atoms determined by total H_2–O_2 titration.
[d] Conditions were 10 Torr C_2H_4, 200 Torr H_2, 0.2 Torr CO and 373–433 K.
[e] Reaction conditions were 5–40 Torr C_2H_4, 200 Torr H_2, 0.2 Torr CO and 403 K.
[f] Reaction conditions were 10 Torr C_2H_4, 140–540 Torr H_2, 0.2 Torr CO and 403 K.
[g] Reaction conditions were 10 Torr C_2H_4, 200 Torr H_2, 0.2–0.9 Torr CO and 403 K.

insensitive. The CO pressure must be stated when reporting TOFs for ethylene hydrogenation poisoned by CO, because a change in CO pressure has a significant influence on the measured rate (see below).

The influence of temperature on the overall reaction rate was measured at 10 Torr C_2H_4, 100 Torr H_2, 0.2 Torr CO, and 373–423 K. At these conditions, all conversions were ⩽10% and verified to be free of mass- and heat-transfer artifacts by the Madon–Boudart test [19]. Apparent activation energy measured at similar pressure conditions (but slightly lower temperatures) in the absence of CO on Pt/SiO_2 catalysts have been reported to be 8–12 kcal mol^{-1}. The apparent activation energy for the CO-poisoned ethylene hydrogenation was ∼20 kcal mol^{-1} for supported catalysts, whereas the Pt powder activation energy was ∼14 kcal mol^{-1}. The Al_2O_3-supported Pt and 0.62% Pt(7.1 nm)/SBA-15 catalysts had an apparent activation energy of 22 kcal mol^{-1}. Arrhenius plots for catalysts are shown in Fig. 1. The values of the apparent activation energies are compiled in Table 2. The same catalysts had apparent activation energies ranging from 8 to 12 kcal mol^{-1} in the absence of CO at 273–323 K [2,3].

Apparent reaction orders in ethylene, hydrogen, and CO have been measured for all catalysts; these values are compiled in Table 2. Reaction orders in ethylene, hydrogen, and CO at 403 K are shown in Fig. 2. Reaction orders were ∼ first order in ethylene, ∼1/2 order in H_2, and −1 in CO for all catalysts (regardless of particle size). The inverse first-order dependence of CO (Fig. 2c) suggests that adsorbed CO is the most abundant surface intermediate (*masi*) [20]. Comparison of reaction kinetics in the presence and absence of CO suggests that both ethylene and hydrogen surface chemistry are influenced by adsorbed CO. The H_2 dependence on the overall reaction were 1/2 at all CO pressures, whereas in the absence of CO at slightly lower temperatures (273–323 K), the hydrogen order is reported to be unity [21]. The first-order dependence on H_2 in the absence of CO is related to competitive adsorption between C_2H_4 and H_2, which becomes insignificant in the presence of CO because adsorbed CO displaces H_2 to surface sites inac-

cessible to ethylene. However, in the case of CO and C_2H_4, the adsorption is competitive. The reaction order in ethylene is zero order in the absence of CO near 273 K [22–24] and becomes more negative at higher temperatures (>323 K) [21]. In the presence of CO, the reaction order is first order at 403 K. Under the reaction conditions of this study, the coverage of ethylene was low [25], and the surface was dominated by atop adsorbed CO (see Section 3.3). The pressure dependence in ethylene remains first order for gas-phase pressures of CO ⩾0.2 Torr (Fig. 3), suggesting that the surface chemistry of ethylene at high temperatures in the presence of CO changes from inhibition to a dependence directly proportional to the gas-phase ethylene pressure.

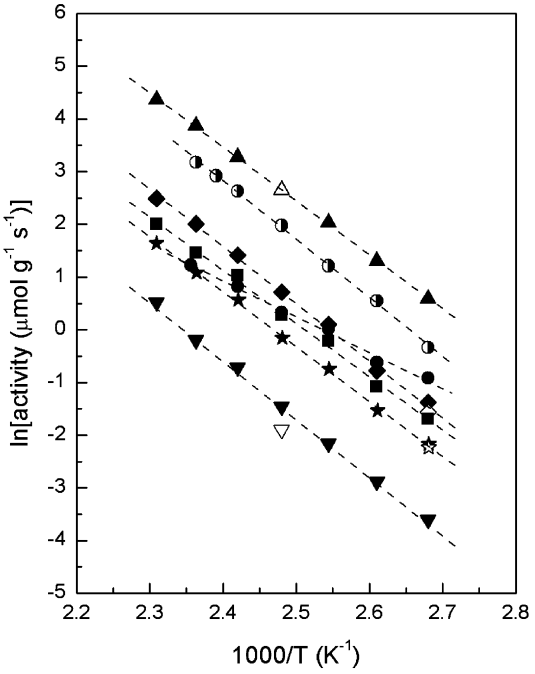

Fig. 1. Arrhenius plot for the hydrogenation of ethylene in the presence of CO. Reaction conditions were 10 Torr C_2H_4, 200 Torr H_2, 0.2 Torr CO and 373–433 K. Apparent activation energies of 20 kcal mol^{-1} are measured in the presence of CO pressures up to 0.9 Torr. (▲) 3.2% Pt/SiO_2; (●) Pt powder; (◆) Pt(1.7 nm)/SBA-15; (■) Pt(2.9 nm)/SBA-15; (★) Pt(3.6 nm)/SBA-15; (▼) Pt(7.1 nm)/SBA-15; (◑) Pt/Al_2O_3.

3.3. *In situ diffuse reflectance spectroscopy under reaction conditions*

The hydrogenation of ethylene under reaction conditions (10 Torr C_2H_4, 100 Torr H_2, 1 Torr CO) was monitored in the diffuse reflectance cell to probe the surface under reaction conditions. Fig. 4 presents a DRIFTS spectrum of a 2.69% Pt(2.9 nm)/SBA-15 catalyst under reaction conditions at 403 K. The rate determined in the DRIFTS cell under these conditions was $\sim 1 \times 10^{-2}$ s^{-1}. Assuming differential operation using ∼10 mg of catalyst, the estimated conversion in this DRIFTS cell was 0.001%. The only adsorbed species under reaction conditions was linear-bonded CO; the band position was red-shifted relative to CO adsorbed on a clean surface at the same temperature [15]. No surface species are observed under reaction conditions at 300 and 403 K for the unpoisoned reaction (spectra not shown), in agreement with previous results from a Pt/Cabosil catalyst [21]. The lack of an ethylidyne peak is most likely due to the high H_2:ethylene ratio (= 10) used and the low ethylene coverage expected at these temperatures.

4. Discussion

4.1. *Comparison of unpoisoned and CO-poisoned ethylene hydrogenation kinetics*

Steady-state activities and TOFs for the hydrogenation of ethylene in the presence of 0.5 Torr CO are compiled in Table 2. Ethylene hydrogenation rates ranged from 1.7 to

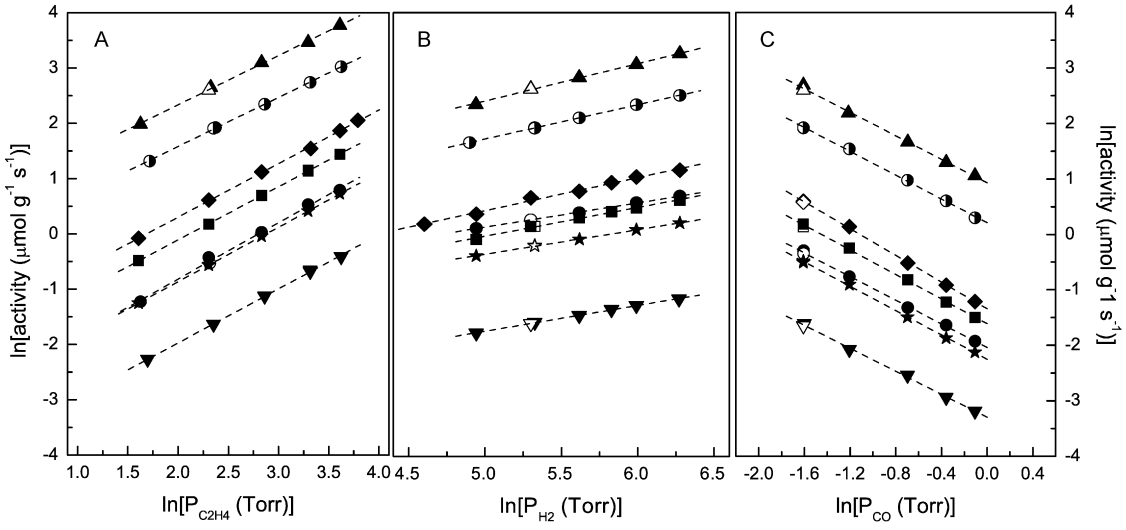

Fig. 2. Reaction orders in (A) C_2H_4, (B) H_2 and (C) CO during C_2H_4 hydrogenation in the presence of CO. Reaction conditions were (A) 5–40 Torr C_2H_4, 200 Torr H_2, 0.2 Torr CO and 403 K; (B) 10 Torr C_2H_4, 140–540 Torr H_2, 0.2 Torr CO and 403 K; and (C) 10 Torr C_2H_4, 200 Torr H_2, 0.2–0.9 Torr CO and 403 K. (▲) 3.2% Pt/SiO_2; (●) Pt powder; (◆) Pt(1.7 nm)/SBA-15; (■) Pt(2.9 nm)/SBA-15; (★) Pt(3.6 nm)/SBA-15; (▼) Pt(7.1 nm)/SBA-15; (◑) Pt/Al_2O_3.

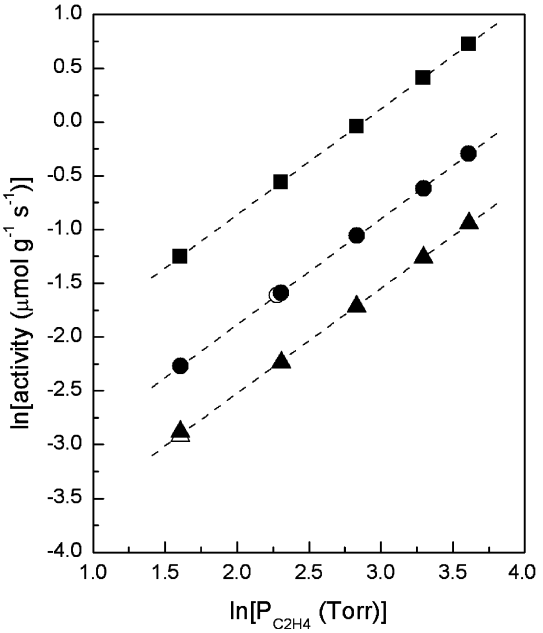

Fig. 3. Reaction orders in C_2H_4 during C_2H_4 hydrogenation in (■) 0.2 Torr, (●) 0.5 Torr and (▲) 0.9 Torr CO on 0.6% Pt(3.6 nm)/SBA-15. Reaction conditions were 5–40 Torr C_2H_4, 200 Torr H_2, stated CO pressure and 403 K.

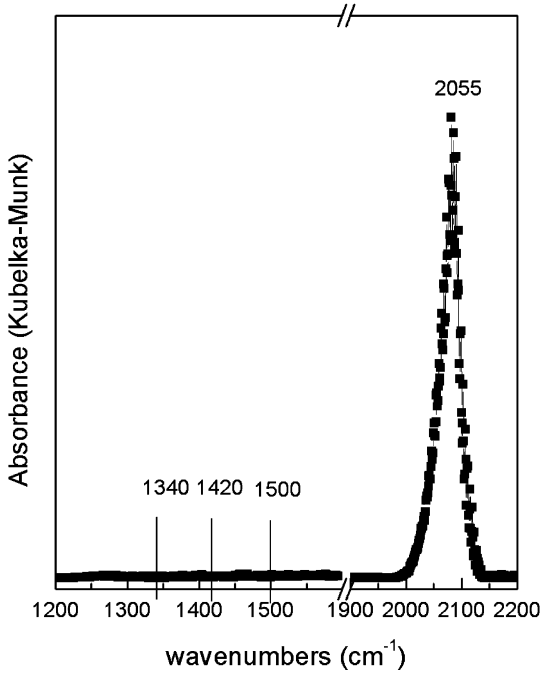

Fig. 4. *In situ* DRIFTS spectra of C_2H_4 hydrogenation (10 Torr C_2H_4, 100 Torr H_2) at 403 K in the presence of 1 Torr CO on 2.69% Pt(2.9 nm)/SBA-15. The frequency for linear-bound CO is 2055 cm^{-1}, peaks associated with ethylidyne (∼1340 cm^{-1}), di-σ bonded (1420 cm^{-1}) ethylene and π-bonded ethylene (∼1500 cm^{-1}) are absent from the surface during catalytic turnover.

3.5×10^{-2} s^{-1} at standard conditions. Extrapolated rates at standard pressure conditions in the absence of CO to 403 K are ∼200 s^{-1}. Previous work demonstrated that only ppm quantities of CO are necessary to completely deactivate a Pd/charcoal catalyst for ethylene hydrogenation [26]. Chen et al. [27,28] have shown that CO is significantly less influential on a Pt(8 nm)/SiO_2 during benzene hydrogenation at 298 K; a CO pressure ⩾30 Torr was required for complete poisoning of hydrogenation. This result differs considerably from that for ethylene hydrogenation in the presence of CO, where catalysts were not active until the temperature was ⩾353 K, and low CO pressures (⩽0.1 Torr) completely poisoned room temperature hydrogenation. Scanning tunneling microscopy studies have shown that the presence of adsorbed CO on Pt(111) leads to the formation of static structures and results in no H_2–D_2 exchange at room temperature [29]. A plausible mechanism for CO poisoning is hindrance of adsorbate mobility, a critical component for catalytic turnover [30]. The influence of CO on ethylene hydrogenation is complex; adsorbate segregation may play a key role and different types of active sites are apparently available on the surface.

4.2. *Effect of CO on the apparent activation energy*

The second consequence of the addition of CO addition was a doubling of the apparent activation energy, which increased from ∼10 to ∼20 kcal mol^{-1} in the presence of 0.2 Torr CO. This doubling of the apparent activation energy was also observed on a Pt(111) single crystal in the presence of 1 Torr CO [7,10]. The gas-phase pressure of CO had little influence on the measured value of the apparent activation energy; in 0.3, 0.5, and 0.9 Torr CO, apparent activation energies of 20.6, 20.1, and 20.8 kcal mol^{-1} (respectively) were measured. Similarly, the apparent activation energy for cyclohexene hydrogenation on Pt(111) doubled in the presence of 0.015 Torr CO [31]. Butt and co-workers found that the apparent activation energy for methylcyclopropane hydrogenolysis increased with CO coverage on a Pt/Al_2O_3 catalyst [32], which may reflect the increasing influence of CO in progressively displacing the reaction to less favorable sites. In a separate study of the same reaction on Pd/SiO_2 [33,34], the authors found the opposite trend—the apparent activation energy decreasing with the addition of CO ($\theta \leqslant 0.5$). In the case of Pd, the authors suggested that low levels of CO immediately remove a population of high activation energy sites from the reaction, although the TOF for *n*-butane formation is an order of magnitude lower than the rate on a clean surface. In a separate study, the apparent activation energy tripled in the presence of CO (1000 ppm) during plug-flow microreactor studies of ethylene hydrogenation on Pd/SiO_2 [35]. It appears that a small amount of CO is sufficient to block most of the active sites for ethylene hydrogenation.

4.3. *CO dominates surface chemistry: C_2H_4–CO competitive adsorption and H_2 surface site distinction*

Reaction orders in C_2H_4 and H_2 were ∼0 and 1/2, respectively, in the absence of CO at low temperatures (<300 K) [3,21], suggesting saturation of the surface with ethylene and gas-phase hydrogen in equilibrium with surface H atoms adsorbed to sites not accessible to ethylene. It is proposed that the distinction between sites is purely steric and not energetic (although a combination of both cannot be ruled out). At higher

temperatures (>340 K), in the absence of CO, the reaction order in hydrogen approaches unity, and the ethylene coverage decreases as both species begin to adsorb to the same type of site. In the presence of CO, the reaction order in hydrogen remains $\sim 1/2$ while the ethylene dependence becomes first order, suggesting that C_2H_4 and CO compete for the same adsorption sites. H_2 is able to adsorb and dissociate on a CO-covered surface because of the availability of adsorption sites that cannot be accessed by CO or ethylene due to steric reasons or more complicated co-adsorption (adsorption-assisted desorption) phenomena. Vacuum and high pressure studies of CO–H_2 co-adsorption have suggested that both adsorbates segregate into islands, in which the local coverage within CO islands is near saturation coverage ($\theta = 0.68$ ML) [36]. These locally high CO coverage regions cause a substantial decrease in CO desorption energy ($\sim$30 kcal mol^{-1} at low coverage to $\sim$10 kcal mol^{-1} at saturation) [37]. Gland and co-workers [37] have shown that the hydrogen-induced displacement of CO has an apparent activation energy of $\sim$11 kcal mol^{-1} above room temperature. If the heat of adsorption of H_2 is greater than the CO desorption energy at saturation, then hydrogen can displace the more weakly bound CO [37]. The differential heat of adsorption of H_2 at saturation on Pt powder measured by microcalorimetry was 13 kcal mol^{-1} [38]; this is greater than the previously reported $\Delta H_{\mathrm{ads,CO}}$ ($\theta = \theta_{\max}$) (-10 kcal mol^{-1}) [39], and in the present case with hydrogen in 1000-fold excess (relative to CO), hydrogen should displace CO from the surface. However, kinetic and infrared spectroscopy measurements suggest that rather than displacing CO, H_2 adsorbs on sites available on a CO-covered surface on which additional CO is unable to adsorb due to steric hindrance of adjacent CO. The formation of CO islands that presumably would open up small ensembles of clean Pt atoms for H_2 dissociation is discounted, because the measured ethylene reaction order is unity for the Pt/SBA-15, and these small clean ensembles would represent a small fraction of surface capable of high-temperature ethylene hydrogenation behavior; that is, ethylene and hydrogen adsorption would be competitive, leading to ethylene and hydrogen partial pressure dependencies different from those observed experimentally.

The influence of CO on ethylene adsorption on Pt has been studied to a lesser extent, but the observed ethylene adsorption kinetics suggest that CO competes with ethylene for surface sites, and kinetic studies on clean Pt/SiO_2 catalysts in the absence of CO demonstrate different kinetics (ethylene inhibits H_2 adsorption). A recent scanning tunneling microscopy study of CO adsorption on a Pt(111) surface precovered with C_2H_4 and H_2 at room temperature demonstrated that densely-packed ($\theta_{\mathrm{CO}} = 0.68$ ML [36]), large mixed C_2H_4–CO unit cells exist with H atoms apparently capable of diffusing within the unit cell [40]. The authors suggested that the rate of H_2 diffusion in the densely packed adlayer is inhibited but not eliminated, suggesting that turnover will occur when hydrogen and ethylene are located on adjacent sites. The integrity of this adlayer may be diminished or less well defined under the high-temperature reaction conditions used in this study, where diffusion is more facile. Sum frequency generation (SFG) surface vibrational spectroscopy studies of C_2H_4/CO co-adsorption on Pt(111) under hydrogenation conditions has demonstrated that linear-bound CO and ethylidyne are present on the surface. A significant interaction between neighboring ethylidyne and CO molecules is likely, as indicated by the red shift of the linear-bound CO vibration after co-adsorption [7]. The most plausible explanation for the increased ethylene pressure dependence is a direct competition between CO and ethylene for surface sites. Only as the pressure is increased can ethylene displace CO from the compressed, mixed adlayer to adsorb and react with H_2 to form ethane. Therefore, the state of the adsorbate-covered surface may be very complex with islands of pure CO and a mixed C_2H_4–CO adlayer, which are sufficiently open to enable dissociative adsorption of hydrogen and diffusion of H atoms in the adlayers. Pure H adlayers are not believed to exist on the surface because the reaction order in hydrogen is $\sim 1/2$, and if patches of a H-covered surface existed, then competitive adsorption between ethylene and hydrogen would occur on this fraction of the surface. This situation would be reflected in a H_2 reaction order $> 1/2$. Table 2 shows that the reaction order in H_2 is $> 1/2$ on the small Pt particles (1–2.7 nm), which may suggest that a small percentage of ethane formation occurs through a competitive mechanism or a smaller fraction of three-fold hollow sites, the preferred adsorption site of H_2 [41]. In fact, H_2 dependencies at room temperature on the same catalyst are $> 1/2$, whereas the H_2 reaction orders on the larger particles are $\sim 1/2$ in the absence of CO [3]. Chen and co-workers [27,28] have identified three types of hydrogen adsorption sites on a Pt/SiO_2 catalyst with Pt particles with a mean diameter of 8 nm. They suggest that the lower benzene hydrogenation activity of a supported Pt catalyst in the presence of CO is related to the elimination of the most reactive low-coordination sites for H_2 activation due to CO adsorption at these sites [28].

4.4. A noncompetitive ethylene hydrogenation mechanism in the presence of CO can explain the doubling of apparent activation energy and partial pressure dependencies

A mechanism in the presence of CO is proposed and the corresponding rate expression derived in Appendix A. A noncompetitive (with respect to ethylene and hydrogen) mechanism with the incorporation of an equilibrated CO adsorption–desorption step is sufficient to describe the kinetics of ethylene hydrogenation in the presence of CO. Noncompetitive mechanisms are possible when adsorption of a reactant requires multiple sites and the maximum surface coverage of the reactant is reached before all sites are occupied, but does not preclude adsorption of smaller molecules on the remaining isolated vacant sites. The effect of noncompetitive adsorption on the hydrogenation of propylene and isobutylene has been documented [42]. For Pt, atop sites represent the preferential adsorption site for both π-bonded ethylene and CO [15,43,44]. This competition for the same type of active site was confirmed by transient pulse methods; the introduction of additional hydrocarbon led to an increase in the CO desorption rate and *vice versa* [45,46].

Diffuse reflectance infrared measurements of ethylene hydrogenation at standard conditions (Fig. 4) confirmed that the surface is dominated by linear-bound CO species, with no evidence of π-bonded C_2H_4, ethylidyne, or the half-hydrogenated ethyl (C_2H_5) species. The Pt surface under ethylene hydrogenation conditions (without CO) is covered with carbonaceous materials, primarily ethylidyne. Radioisotope ^{14}C ethylene studies [47] demonstrate that ethylidyne reacts to form ethane six orders of magnitude slower than π-bonded C_2H_4. In the presence of CO and the high H_2:C_2H_4 ratios used in this study, the coverage of all potential ethylene-derived intermediates is low (at least below the detection limit of the DRIFTS experiment). The proposed reactive intermediate, π-bonded ethylene, is present as only 4% of a monolayer under reaction conditions (35 Torr C_2H_4, 100 Torr H_2, 295 K) [48], and the coverage of such species is significantly lower when co-adsorbed with CO, as reported recently [15]. CO influences the overall reaction rate by inhibiting ethylene adsorption and/or displacing adsorbed ethylene from the surface. The rate-determining step (the addition of hydrogen to the half-hydrogenated intermediate) is unchanged by the presence of CO in the gas phase, although the kinetic dependence on ethylene changes due a change in the *masi*. Kinetic (Figs. 2 and 3) and spectroscopic (Fig. 4) measurements suggest that CO is the *masi*, and thus CO must desorb to allow ethylene adsorption and hydrogenation. The particle size insensitivity to poisoning by CO suggests that the rate-determining step requires only one or two sites to convert ethylene to ethane, supporting the proposed mechanism in which conversion can occur on a single site adjacent to a H atom source, namely S–H (see Appendix A). Both π-bonded ethylene and ethyl stability is maximized on atop sites [49], and H atom diffusion on the surface is facile at these temperatures. The energetic penalty paid for CO removal is $\sim$10 kcal mol^{-1}, in agreement with previous studies on the heat of adsorption for CO on Pt surfaces [39,50]. The doubling of the apparent activation energy can be explained in terms of an equilibrium between gas-phase CO and a CO-saturated Pt surface (Appendix A, Eq. (5)). The true activation energy (E_{true}) for ethylene hydrogenation remains the same because the rate-determining step does not change, and only the *apparent* activation energy increases. The apparent activation energy in the absence of CO, E_{app} depends on E_{true} and the enthalpy of adsorption of ethylene and hydrogen, respectively, whereas in the presence of CO, $E_{app,CO}$ is equal to E_{app} plus the contribution of the enthalpy of adsorption of CO ($\Delta H_{ads,CO}$). The apparent activation energy for the hydrogenation of ethylene on clean Pt ranges from 8 to 12 kcal mol^{-1} [3,51]; including the heat of adsorption of CO at saturation coverage ($\sim$10 kcal mol^{-1}), $E_{app,CO}$ increases to $\sim$20 kcal mol^{-1}, in agreement with experimental observations. A similar argument has been proposed for the increase in apparent activation energy for ethylene hydrogenation in the presence of CO on Pd/SiO_2 catalysts [35]. A mechanism based on competitive H_2 adsorption could not reproduce the observed pressure dependencies and predict a doubling of the apparent activation energy.

4.5. Influence of particle size on poisoning of ethylene hydrogenation by CO

Kinetic studies demonstrated that the rate of ethylene hydrogenation is independent of the arrangement of the underlying metal atoms and thus is considered a structure-insensitive reaction [49,52]. One proposal for this insensitivity is the formation of an alkyl–metal "complex" [53] that effectively eliminates the surface's identity, with the resultant ethylidyne becoming the active site for hydrogenation of ethylene by weakly binding incoming ethylene in a π-bonded form and shuttling H atoms from the Pt surface to the weakly bound ethylene species. Other studies have proposed various possibilities for the structure insensitivity, each of which involves either a one-site or a two-site mechanism [49,52–55].

The influence of particle size on the ethylene hydrogenation TOF for the poisoned (0.5 Torr CO) and unpoisoned reaction is shown in Fig. 5; the rate follows a trend in which larger particles are influenced more by the presence of CO, although the difference in rate on small and large particles is only a factor of two compared with the rate of the unpoisoned reaction, which is independent of particle size (see Fig. 5). A significant number of reports suggest that ethylidyne formation is favored on larger Pt particles. The formation of ethylidyne on more open Pt single crystals with coordination numbers similar to those on small Pt crystallites (1–2.5 nm) has been observed less frequently due to the formation and stabilization of more highly dehydrogenated species [56,57]. The formation of this ethylidyne layer is structure-sensitive [58], but its presence is not critical for catalysis on smaller particles [23,59]; however,

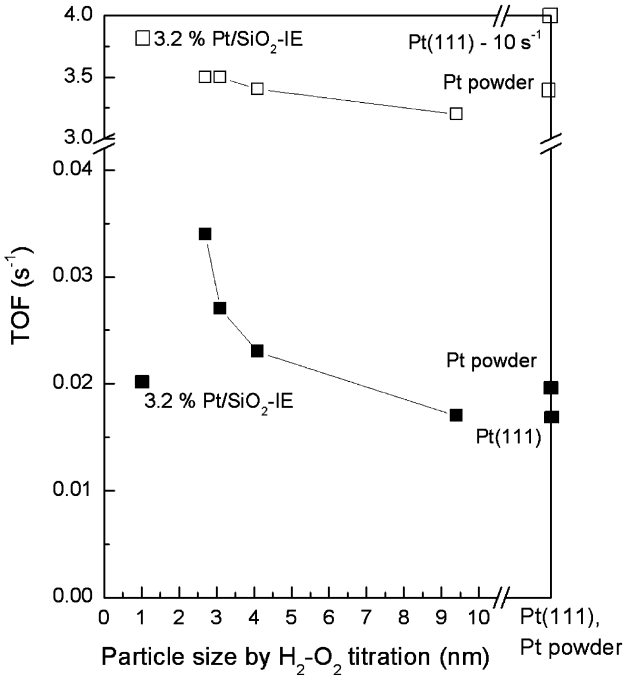

Fig. 5. Influence of Pt particle size on the TOF for ethylene hydrogenation in the absence or presence of CO. (□) Reaction conditions were 10 Torr C_2H_4, 100 Torr H_2, 0 Torr CO and 298 K. (■) Reaction conditions were 10 Torr C_2H_4, 100 Torr H_2, 0.5 Torr CO and 403 K.

whether this is true for larger particles is not known. This may be of particular importance if ethylidyne is necessary for ethylene turnover, because ethylidyne is believed to require the 3-fold symmetry of (111) facets rather than random trimer assemblies of Pt atoms [60]. The presence of adsorbed CO would have a greater affect on catalysts composed of larger crystallites ($\geqslant$5 nm), because adsorbed CO would inhibit ethylidyne formation by breaking up 3-fold hollow sites.

The results are not conclusive (although a significant amount of single crystal work supports this claim), but the hydrogenation of ethylene on larger crystallites may *require* the ethylidyne adlayer, the formation of which would be suppressed in the presence of adsorbed CO due to site blocking and dilution of favored 3-fold hollow sites for adsorption. This layer may not be necessary on small Pt nanoparticles because of the high concentration of low-coordination atop sites, the preferred adsorption site for π-bonded ethylene [61]. Rates of the poisoned ethylene hydrogenation reaction on large Pt particle catalysts—Pt(7.1 nm)/SBA-15 and Pt powder—are in good agreement with the rate measured on Pt(111) [6,7,10], confirming that large particles are slightly more sensitive to poisoning by CO for the hydrogenation of ethylene. The apparent structure-insensitivity of ethylene hydrogenation is upheld in the presence of CO, even though infrared measurements suggest that the nature of CO adsorption changes with Pt particle sizes. The particle size insensitivity to poisoning by CO suggests that the rate-determining step requires only one or two sites; the same scenario postulated for the "clean" reaction.

4.6. Comparison of CO-poisoned ethylene hydrogenation rates with previously reported Pt catalysts

The poisoning of ethylene hydrogenation by CO on a number of different Pt-based catalysts has been studied by Somorjai and coworkers [6,8–10,28]. TOFs corrected to standard conditions are compiled in Table 3. Rates vary by three orders of magnitude at identical poisoning conditions. The reported ethylene hydrogenation rate in the presence of ~0.5 Torr CO at 403 K on a Pt(111) single crystal is 1.7×10^{-2} s^{-1}, which is ~5 orders of magnitude lower than the rate in the case of the unpoisoned reaction [62]. The presence of 1 Torr CO in the feed leads to a doubling of the apparent activation energy on Pt(111) [6,7,10]. Rates on lithographically generated SiO_2- and Al_2O_3-supported Pt nanowire arrays are an order of magnitude more active than Pt/SBA-15 and the Pt single crystal. In the case of the nanowire arrays, the apparent activation energy in the absence and presence of 0.3 Torr CO is ~13 and ~21 kcal mol^{-1}, respectively. For the Pt nanoparticle arrays on SiO_2 and Al_2O_3 supports, the TOFs are three orders of magnitude higher than the Pt/SBA-15 catalysts. The authors suggest that increased activity of these nanoparticle arrays is due to sites at the metal–oxide interface that are not poisoned by CO [8,9]. Correction of the nominal TOF using simple geometric arguments that account only for the sites located at this metal–oxide interface demonstrate that the TOF (7.1 s^{-1}) is similar to the unpoisoned catalyst (7.3 s^{-1}) [8]. The apparent activation energy on the lithography generated nanoparticle array catalyst increased by only ~2 kcal mol^{-1} on CO addition. The authors suggested the enhanced activity of the nanoparticle arrays is due to the rapid hydrogenation of CO adsorbed to these interface sites [63]. The rate of CO hydrogenation is enhanced at the Pt–TiO_2 interface [64], but no such enhancement was observed for CO hydrogenation on Pt–SiO_2 [65,66]. A nominal TOF for CO hydrogenation of 10^{-5} s^{-1} is estimated (using the kinetics reported in Refs. [65,66]) for conditions similar to those used in this study (1 Torr CO, 100 Torr H_2, and 473 K). Calculation of the CO hydrogenation TOF based only on metal–oxide interface sites (assuming no structure-sensitivity or enhanced reactivity at the interface), a rate of ~10^{-3} s^{-1} is calculated. This is significantly lower than the olefin hydrogenation rate (~7 s^{-1}) in the presence of CO, suggesting that the enhanced activity of the Pt nanoparticle array catalysts is probably due to a reason other than rapid CO hydrogenation.

Table 3
Compilation of C_2H_4 hydrogenation kinetics in the presence of CO on Pt catalysts

Catalyst	C_2H_4 hydrogenation in the presence of CO at standard conditions[a] TOF (s^{-1})	Reference
Pt powder	3.3×10^{-2}	This work
3.2% Pt/SiO_2	3.3×10^{-2}	This work
2% Pt/Al_2O_3	6×10^{-2}	This work
0.6% Pt(1.7 nm)/SBA-15	6.2×10^{-2}	This work
0.77% Pt(2.9 nm)/SBA-15	4.7×10^{-2}	This work
0.6% Pt(3.6 nm)/SBA-15	4×10^{-2}	This work
0.62% Pt(7.1 nm)/SBA-15	2.8×10^{-2}	This work
Pt(111) single crystal[b]	2.8×10^{-2}	[9,10]
28 nm Pt nanoparticle array on Al_2O_3	9	[9]
28 nm Pt nanoparticle array on SiO_2	33	[9]
22 nm Pt nanowire array on Al_2O_3	0.5	[9]
25 nm Pt nanowire array on SiO_2	0.2	[9]
64 nm Pt nanowire array on SiO_2	0.4	[9]

[a] Standard conditions are 10 Torr C_2H_4, 100 Torr H_2, 0.3 Torr CO and 403 K.
[b] The rate of ethylene hydrogenation was extrapolated from 10 Torr C_2H_4, 100 Torr H_2, 1 Torr CO (assuming inverse first order dependence in CO) and 403 K to standard conditions.

5. Conclusion

The kinetics of the hydrogenation of ethylene poisoned by CO was found to differ substantially (~4–5 orders of magnitude) from that of the unpoisoned reaction. The apparent activation energy, ethylene order, and hydrogen order changed in the presence of CO (0.2–1 Torr). In the presence of CO, the reaction rate was first-order in ethylene and 1/2 order in H_2. Kinetic measurements demonstrated that C_2H_4 pressure dependence is invariant with CO pressures >0.2 Torr, suggesting saturation of the surface with CO, leading to the inverse first-order dependence on CO pressure. The apparent activation energies double regardless of particle size and do not change with CO pressure. This increase is a consequence of the adsorption equilibrium maintained between adsorbed and gas-phase CO, not a change in the rate-determining step. The only surface species observed by *in situ* diffuse reflectance spectroscopy during the hydrogenation of ethylene in the presence of CO was linear-

bound CO, the frequency of which was red-shifted relative to CO adsorption on a clean catalyst surface. The inclusion of a CO adsorption–desorption equilibrium to the noncompetitive Horiuti–Polanyi mechanism for ethylene hydrogenation reproduced the experimentally observed kinetics. The hydrogenation of ethylene on Pt catalysts was structure-insensitive in the absence and presence of CO.

Acknowledgments

This work was supported by the Director, Office of Science, Office of Advanced Scientific Computing Research, Office of Basic Energy Sciences, Materials Sciences and Engineering Division of the U.S. Department of Energy under contract DE-AC02-05CH11231. The authors thank Professor M.A. Vannice, Pennsylvania State University for donating the 3.2% Pt/SiO_2 catalyst and Dr. Samrat Mukherjee for its preparation. They also thank the Exxon Research and Developmental Laboratory for donating the Pt/Al_2O_3 sample. R.M.R. thanks the Ford Motor Company for financial support through a graduate fellowship administered by the Berkeley Catalysis Center.

Appendix A. Incorporating CO into a noncompetitive ethylene hydrogenation mechanism

Horiuti and Polanyi proposed a mechanism for the hydrogenation of ethylene over Ni catalysts, in which ethylene is hydrogenated to ethane through a half-hydrogenated intermediate [17]. In this competitive mechanism, ethylene and hydrogen compete for the same type of site. This mechanism does not capture the macroscopic reaction kinetics at low temperatures. A noncompetitive variant of the Horiuti–Polanyi mechanism has been proposed in which hydrogen and ethylene adsorption on separate types of sites can explain the low-temperature macroscopic kinetics, but this variant is incapable of reproducing high-temperature kinetics. Therefore, both mechanisms are unable to reproduce the experimental kinetics over a range of conditions (ethylene:H_2 ratios and temperature). At high temperatures (403 K) and low ethylene pressures (5–40 Torr) used in this work, by combining results from steady-state kinetic and temperature-programmed measurements, deuterium tracing experiments, and microkinetic modeling, Dumesic et al. showed that a H_2-activated noncompetitive–competitive mechanism can reproduce the experimental kinetic data [27]. In this appendix, a rate expression that accounts for the observed kinetics in the presence of CO is derived by the addition of a CO adsorption–desorption equilibrium step to the noncompetitive mechanism.

The noncompetitive Horiuti–Polanyi ethylene hydrogenation mechanism consists of four elementary steps:

1. Non-competitive hydrogen adsorption: $H_2 + 2S \rightleftharpoons 2H\text{–}S$.
2. Ethylene adsorption: $C_2H_4 + * \rightleftharpoons C_2H_4*$.
3. First surface hydrogenation reaction: $C_2H_4* + H\text{–}S \rightleftharpoons C_2H_5* + S$.
4. Surface reaction of half-hydrogenated intermediate: $C_2H_5* + H\text{–}S \rightarrow C_2H_6 + * + S$.

Steps 1–3 are quasi-equilibrated ($\rightleftharpoons$), and step 4 is rate-determining. Steps 1–4 constitute a catalytic cycle, a single turnover of ethylene to ethane, and regeneration of the * site and S site, respectively. Surface sites denoted by * are adsorption sites for hydrocarbons only, whereas sites denoted by S are for the adsorption of hydrogen only. The distinction between * and S is due purely to steric considerations. In the absence of CO, the surface coverage of carbonaceous species is high at low temperatures but decreases at higher temperatures (>340 K), due to poor adsorption thermodynamics. Adsorption in a π-bonded or di-σ configuration requires at least a single site (*) or a pair (*–*) and potentially more due to steric considerations [27]. Hydrogen atoms adsorb in three-fold hollow sites on Pt(111) [41], and if ethylene adsorbs randomly on the surface, then hydrogen adsorption sites exist on the ethylene-covered surface because pairs of threefold sites near ethylene are sterically blocked from adsorbing another ethylene molecule [27].

Formulation of a rate expression assuming the foregoing sequence of elementary steps with adsorbed carbonaceous species as the most abundant * species and adsorbed hydrogen saturating the S sites leads to a mechanism consistent with low-temperature kinetics: zero-order ethylene and reversible half-order hydrogen kinetics. The coverage of hydrogen ($\theta_{H\text{–}S}$) is determined by step 1 and scales with $P_H^{1/2}$ ($\theta_{H\text{–}S} = K_{H\text{–}S}^{1/2} P_{H_2}^{1/2} \theta_S$), being independent of the ethylene pressure due to the two-site mechanism. A competitive (S and * are identical) mechanism leads to a rate expression that is unable to capture the experimentally observed kinetics at low temperature.

The introduction of CO leads to different experimental kinetics than those observed in the hydrogenation of ethylene in the absence of adsorbed CO. As shown in Table 2, the reaction order in C_2H_4 is unity, 1/2 in H_2 and −1 in CO. Fig. 3 demonstrates that the reaction order in ethylene is first order regardless of CO pressure. The hydrogen reaction order remains ∼1/2, regardless of CO or ethylene pressure (not shown). This leads to the conclusion that adsorption of H_2 and C_2H_4 is noncompetitive at high temperatures in the presence of CO, in contrast with the competitive nature of C_2H_4 and H_2 adsorption in the absence of CO at similar temperatures; for example, Cortright et al. measured a −0.43 order dependence for C_2H_4 in the absence of CO on a Pt/SiO_2 catalyst at 336 K [23]. The adsorption of CO and ethylene is competitive, with the rate of hydrogenation directly proportional to the ethylene pressure and adsorbed CO dominating the surface under reaction conditions (see Figs. 3 and 4). The adsorption of CO on the surface is governed by the following equilibrium:

5. CO adsorption: $CO + * \rightleftharpoons CO*$.

The coverage of CO is defined as $\theta_{CO} = K_{CO} P_{CO} \theta_*$, where K_{CO} is the equilibrium adsorption constant and θ_* is the fraction of empty * sites. Retaining the uncompetitive mechanism with the addition of a CO adsorption–desorption equilibrium step leads to the half-order H_2 dependency and inverse first-order CO dependency if CO is the most abundant surface

species on * type sites (as suggested by infrared measurements; see Fig. 4). The rate of C_2H_6 formation is determined by the rate-determining addition of adsorbed hydrogen to the half-hydrogenated intermediate, $r = k_{app}\theta_{C_2H_5*}\theta_{H–S}$, and the complete mechanism (steps 1–5) can be used to derive a power rate law, $r = k_{app}P_{C_2H_4}P_{H_2}^{1/2}P_{CO}^{-1}$, assuming that [CO*] and [H–S] are the most abundant species on their respective types of sites. The observed rate expression correctly predicts the experimentally observed pressure dependencies and a doubling of the apparent activation energy (as explained in Section 4.4).

References

[1] R.M. Rioux, H. Song, M. Grass, S. Habas, K. Niesz, J.D. Hoefelmeyer, P. Yang, G.A. Somorjai, Top. Catal. 39 (2006) 167.
[2] R.M. Rioux, H. Song, J.D. Hoefelmeyer, P. Yang, G.A. Somorjai, J. Phys. Chem. B 109 (2005) 2192.
[3] H. Song, R.M. Rioux, J.D. Hoefelmeyer, R. Komor, K. Niesz, M. Grass, P.D. Yang, G.A. Somorjai, J. Am. Chem. Soc. 128 (2006) 3027.
[4] T. Teranishi, M. Hosoe, T. Tanaka, M. Miyake, J. Phys. Chem. B 103 (1999) 3818.
[5] Y. Wang, Chem. Mater. 12 (2000) 1622.
[6] P. Chen, K.Y. Kung, Y.R. Shen, G.A. Somorjai, Surf. Sci. 494 (2001) 289.
[7] P. Chen, S. Westerberg, K.Y. Kung, J. Zhu, J. Grunes, G.A. Somorjai, Appl. Catal. A Gen. 229 (2002) 147.
[8] A.M. Contreras, J. Grunes, X.-M. Yan, A. Liddle, G.A. Somorjai, Catal. Lett. 100 (2005) 115.
[9] A.M. Contreras, J. Grunes, X.-M. Yan, A. Liddle, G.A. Somorjai, Top. Catal. 39 (2006) 123.
[10] J. Grunes, J. Zhu, M.C. Yang, G.A. Somorjai, Catal. Lett. 86 (2003) 157.
[11] M.L. Hair, Infrared Spectroscopy in Surface Chemistry, Dekker, New York, 1967, p. 256.
[12] L.H. Little, Infrared Spectra of Adsorbed Species, Academic Press, New York, 1966, p. 125.
[13] M. Frank, M. Bäumer, R. Kühnemuth, H.J. Freund, J. Vac. Sci. Technol. A 19 (2001) 1497.
[14] G. Blyholder, J. Phys. Chem. 68 (1964) 2772.
[15] R.M. Rioux, J.D. Hoefelmeyer, M. Grass, H. Song, K. Niesz, P. Yang, G.A. Somorjai, Langmuir 24 (2008) 198.
[16] I. Horiuti, M. Polanyi, Trans. Faraday Soc. 30 (1934) 1164.
[17] H. Song, F. Kim, S. Connor, G.A. Somorjai, P.D. Yang, J. Phys. Chem. B 109 (2005) 188.
[18] J.E. Benson, M. Boudart, J. Catal. 4 (1965) 704.
[19] R.J. Madon, M. Boudart, Ind. Eng. Chem. Fundam. 24 (1982) 438.
[20] M. Boudart, AIChE J. 18 (1972) 465.
[21] R.D. Cortright, S.A. Goddard, J.E. Rekoske, J.A. Dumesic, J. Catal. 127 (1991) 342.
[22] G.C. Bond, J.J. Phillipson, J.M. Winterbottom, P.B. Wells, Trans. Faraday Soc. 60 (1964) 1847.
[23] J.E. Rekoske, R.D. Cortright, S.A. Goddard, S.B. Sharma, J.A. Dumesic, J. Phys. Chem. 96 (1992) 1880.
[24] J.C. Schlatter, M. Boudart, J. Catal. 24 (1972) 482.
[25] J.A. Dumesic, D.F. Rudd, L.M. Aparicio, J.E. Rekoske, A.A. Treviño, The Microkinetics of Heterogeneous Catalysis. ACS Professional Reference Book, Am. Chem. Soc., Washington, DC, 1993.
[26] D. Pope, D.S. Walker, R.L. Moss, J. Catal. 28 (1973) 46.
[27] C.S. Chen, J.H. Lin, H.W. Chen, Appl. Catal. A Gen. 298 (2006) 161.
[28] C.S. Chen, J.H. Lin, H.W. Chen, C.Y. Wang, Catal. Lett. 105 (2005) 149.
[29] D.C. Tang, Ph.D. Dissertation, University of California, Berkeley, 2005.
[30] G.A. Somorjai, Nature 430 (2004) 730.
[31] M.C. Yang, R.M. Rioux, G.A. Somorjai, J. Catal. 237 (2006) 255.
[32] J.B. Butt, C.L.M. Joyal, J. Chem. Soc. Faraday Trans. 86 (1990) 2911.
[33] D.E. Damiani, J.B. Butt, J. Catal. 94 (1985) 203.
[34] I. Önal, J.B. Butt, J. Chem. Soc. Faraday Trans. 78 (1982) 1887.
[35] H. Zea, K. Lester, A.K. Datye, E. Rightor, R. Gulotty, W. Waterman, M. Smith, Appl. Catal. A Gen. 282 (2005) 237.
[36] E.K. Vestergaard, P. Thostrup, T. An, E. Lægsgaard, I. Stensgaard, B. Hammer, F. Besenbacher, Phys. Rev. Lett. 88 (2002) 259601.
[37] J.L. Gland, D.A. Fischer, D.H. Parker, S. Shen, Langmuir 7 (1991) 2574.
[38] B.E. Spiewak, R.D. Cortright, J.A. Dumesic, J. Catal. 176 (1998) 405.
[39] E.G. Seebauer, A.C.F. Kong, L.D. Schmidt, Surf. Sci. 176 (1986) 134.
[40] D.C. Tang, K.S. Hwang, M. Salmeron, G.A. Somorjai, J. Phys. Chem. B 108 (2004) 13300.
[41] K. Christmann, Surf. Sci. Rep. 9 (1988) 1.
[42] G.B. Rogers, M.M. Lih, O.A. Hougen, AIChE J. 12 (1966) 369.
[43] J. Evans, G.S. McNulty, J. Chem. Soc. Dalton Trans. 1 (1984) 79.
[44] M.J. Grogan, K. Nakamoto, J. Am. Chem. Soc. 88 (1966) 5454.
[45] L. Cider, N.H. Schöön, Appl. Catal. 68 (1991) 191.
[46] L. Cider, N.H. Schöön, Appl. Catal. 68 (1991) 207.
[47] S.M. Davis, F. Zaera, B.E. Gordon, G.A. Somorjai, J. Catal. 92 (1985) 240.
[48] P.S. Cremer, X.C. Su, Y.R. Shen, G.A. Somorjai, Catal. Lett. 40 (1996) 143.
[49] P.S. Cremer, X.C. Su, Y.R. Shen, G.A. Somorjai, J. Am. Chem. Soc. 118 (1996) 2942.
[50] R.D. Cortright, J.A. Dumesic, J. Catal. 148 (1994) 771.
[51] J. Horiuti, K. Miyahara, Hydrogenation of Ethylene on Metallic Catalysts, NBS-NSRDS, vol. 13, U.S. Government Printing Office, Washington, DC, 1968.
[52] T.A. Dorling, M.J. Eastlake, R.L. Moss, J. Catal. 14 (1969) 23.
[53] M. Boudart, J. Mol. Catal. 30 (1985) 27.
[54] M. Neurock, R.A. van Santen, J. Phys. Chem. B 104 (2000) 11127.
[55] D.L. Thorn, R. Hoffmann, J. Am. Chem. Soc. 100 (1978) 2079.
[56] N. Sheppard, C.D.L. Cruz, Adv. Catal. 41 (1996) 1.
[57] N. Sheppard, C.D.L. Cruz, Adv. Catal. 42 (1998) 181.
[58] F.B. Passos, M. Schmal, M.A. Vannice, J. Catal. 160 (1996) 118.
[59] T.P. Beebe, J.T. Yates, Surf. Sci. 173 (1986) L606.
[60] D.K. Paul, T.P. Beebe, K.J. Uram, J.T. Yates, J. Am. Chem. Soc. 114 (1992) 1949.
[61] A.L. Backman, R.I. Masel, J. Phys. Chem. 94 (1990) 5300.
[62] F. Zaera, G.A. Somorjai, J. Am. Chem. Soc. 106 (1984) 2288.
[63] K.S. Hwang, M.C. Yang, J. Zhu, J. Grunes, G.A. Somorjai, J. Mol. Catal. A Chem. 204 (2003) 499.
[64] M.E. Levin, M. Salmeron, A.T. Bell, G.A. Somorjai, J. Catal. 106 (1987) 401.
[65] M.A. Vannice, J. Catal. 37 (1975) 449.
[66] M.A. Vannice, J. Catal. 40 (1975) 129.